

Supporting Information

Ruthenium Oxide Coated Ordered Mesoporous Carbon Nanofiber Arrays: A Highly Bifunctional Oxygen Electrocatalyst for Rechargeable Zn–air Batteries

Ziyang Guo,^a Chao Li,^a Wangyu Li,^a Hua Guo,^a Xiuli Su,^a Ping He,^b Yonggang Wang*
^a and Yongyao Xia ^a

a Department of Chemistry and Shanghai Key Laboratory of Molecular Catalysis and Innovative Materials, Institute of New Energy, iChEM (Collaborative Innovation Center of Chemistry for Energy Materials), Fudan University, Shanghai 200433, China.

b Center of Energy Storage Materials & Technology, College of Engineering and Applied Sciences, National Laboratory of Solid State Microstructures, and Collaborative Innovation Center of Advanced Microstructures, Nanjing University, Nanjing 210093, China.

* Corresponding author. Tel & Fax: 0086-21-51630318
E-mail address: ygwang@fudan.edu.cn

Experimental Section

Materials preparation

Synthesis of MCNAs: Poly(propylene oxide)–block–poly(ethylene oxide)–block–poly(propylene oxide) triblock copolymer Pluronic P123 (Mw 5800, EO20PO70EO20) was purchased from Aldrich Corp. Ethanol, phenol and formalin solution (37 wt %) were analytical reagents and purchased from Shanghai Chemical Corp. The resol precursors (Mw < 500) were prepared according to the literature method (ref. S1). All chemicals were used as received without further purification.

The crab shells were calcined in air at 350 °C to remove organic protein and chitin on the surface, and ground into a powder in a mortar. The ordered mesoporous carbon nanofibers were prepared through the combined hard-templating and surfactant self-assembly approach by impregnation of an ethanol solution of resol and triblock copolymer P123 (ref. S2). For a typical procedure, the crab shell skeleton (1.0 g) with channel size of 70 nm was immersed in a homogeneous ethanol solution (16.0 g) containing resol (1.0 g) and P123 (0.5 g). The impregnated composites were evaporated at 25 °C for 6 h, followed by further thermosetting at 100 °C for 24 h. The resulting calcium carbonate/resol/P123 composites were then pyrolyzed in nitrogen at 350 °C for 2 h at a heating rate of 1 °C min⁻¹ to remove the P123 template, and at 5 °C min⁻¹ to 900 °C for 2 h for further carbonization. The obtained calcium carbonate/carbon composites were treated with (6 M) HCl solution to remove the calcium carbonate template, followed by washing with deionized water and ethanol, and drying at 100 °C in air for 24 h.

RuO₂-coated MCNAs preparation: The resulting MCNAs were treated with nitric acid (30%) at 90 °C for 1 h. Next, the acid-treated ordered MCNAs (100 mg) were dispersed in a 0.01 M RuCl₃ solution (50 mL) by ultrasonication. A 0.05 M NaHCO₃ aqueous solution was added slowly to the above solution under stirring until the pH reached 7. After another 2 h of stirring, the sediments were washed with distilled water, and then dried at 80 °C for 8h and heat treated at 120 °C. The as-prepared sample was donated as RuO₂-coated MCNAs.

ref. S1: Y. Meng, D. Gu, F. Q. Zhang, Y. F. Shi, H. F. Yang, Z. Li, C. Z. Yu, B. Tu and D. Y. Zhao, *Angew. Chem., Int. Ed.*, 2005, **44**, 7053–7059.

ref. S2: Y. H. Deng, C. Liu, T. Yu, F. Liu, F. Q. Zhang, Y. Wan, L. J. Zhang, C. C. Wang, B. Tu, P. A. Webley, H. T. Wang and D. Y. Zhao, *Chem. Mater.*, 2007, **19**, 3271–3277.

Physicochemical Characterization

X-ray diffraction (XRD) measurements were performed on a Bruker D8 Focus power X-ray diffractometer with Cu K radiation. SEM investigations were conducted using a JSM-6390 microscope from JEOL. Transmission electron microscopy (TEM) experiments were conducted using a JEOL 2011 microscope (Japan) operated at 200 kV. Nitrogen sorption isotherms were measured at 77 K with a Micromeritics Tristar 3000 analyzer (USA). Specific surface areas were calculated by the Brunauer–Emmert–Teller method. Pore volumes and sizes were estimated from the pore-size distribution curves from the adsorption isotherms using the Barrett–Joyner–Halenda method. X-ray photoelectron spectroscopy (XPS) was

conducted with a Thermo Escalab 250 equipped with a hemispherical analyzer and using an aluminum anode as a source.

Electrochemical characterization

Measurement of Electrocatalytic performances of catalysts towards ORR and OER:

Electrocatalytic ORR and OER measurements were performed in a three-electrode glass cell. The data were recorded using a CHI 660 D bipotentiostat (Shanghai Chen Hua instrument co., LTD, China). The synthesized MCNAs, RuO₂-coated MCNAs and commercial Active Carbon (AC) were directly used as the working electrode for electrochemical characterizations. The reference electrode was an Hg/HgO in 1 M KOH solution, and the counter electrode was a platinum film. The current density was normalized to the geometrical surface area and the measured potentials vs. Hg/HgO were converted to a reversible hydrogen electrode (RHE) scale according to the Nernst equation ($E_{\text{RHE}} = E_{\text{Hg/HgO}} + 0.059 \times \text{pH} + 0.098$). A flow of O₂ was maintained over the electrolyte (0.1 M KOH) during the recording of electrochemical data in order to ensure the O₂/H₂O equilibrium at 1.23 V vs. RHE. Cyclic voltammograms (CVs) were performed with the scan rate at 5 mV s⁻¹, and working electrodes were scanned for several times until stabilization before CV data were collected. The linear sweep voltammograms (LSVs) were conducted with the scan rate of 5 mV s⁻¹. The working electrodes were scanned for several times until the signals were stabilized, then LSV data were collected, corrected for the iR contribution within the cell. The Tafel slope was calculated according to Tafel equation as follows:

$$\eta = b \log(j/j_0)$$

where η denotes the overpotential, b denotes the Tafel slope, j denotes the current density, and j_0 denotes the exchange current density. The onset potentials were determined based on the beginning of the linear region in Tafel plots. The overpotential was calculated as follows:

$$\eta = E \text{ (vs. RHE)} - 1.23$$

considering O_2/H_2O equilibrium at 1.23 V vs. RHE.

On the basis of RDE data, the electron transfer number per oxygen molecule involved in oxygen reduction can be determined by Koutechy-Levich equation (ref. S3 and 4):

$$1/j = 1/j_k + 1/B\omega^{1/2} \quad (1)$$

where j_k is the kinetic current and ω is the electrode rotating rate. B is determined from the slope of the Koutechy-Levich (K-L) plots according to the Levich equation as given below:

$$B = 0.2nF(D_{O_2})^{2/3}v^{-1/6}C_{O_2} \quad (2)$$

where n represents the transferred electron number per oxygen molecule. F is Faraday constant ($F = 96485 \text{ C mol}^{-1}$). D_{O_2} is the diffusion coefficient of O_2 in 0.1 M KOH ($D_{O_2} = 1.9 \times 10^{-5} \text{ cm}^2 \text{ s}^{-1}$). v is the kinetic viscosity ($v = 0.01 \text{ cm}^2 \text{ s}^{-1}$). C_{O_2} is the bulk concentration of O_2 ($C_{O_2} = 1.2 \times 10^{-6} \text{ mol cm}^{-3}$). The constant 0.2 is adopted when the rotation speed is expressed in rpm.

ref. S3: Y. Y. Liang, H. L. Wang, J. G. Zhou, Y. G. Li, J. Wang, T. Regier and H. J. Dai, *J. Am. Chem. Soc.*, 2012, **134**, 3517–3523.

ref. S4: Y. H. Deng, C. Liu, T. Yu, F. Liu, F. Q. Zhang, Y. Wan, L. J. Zhang, C. C. Wang, B. Tu, P. A. Webley, H. T. Wang and D. Y. Zhao, *Chem. Mater.*, 2007, 19, 3271–3277. S. K. Zecevic, J. S. Wainright, M. H. Litt, S. L. Gojkovic and R. F. Savinell, *J. Electrochem. Soc.*, 1997, **144**, 2973-2982.

Preparation of working electrodes: Firstly, the active material (~4 mg for RuO₂-coated MCNAs) was dispersed in 1 mL of water/ethanol (v/v: 2/1). Then, 120 μL Nafion (5 wt% aqueous solution, Sigma Aldrich) was added to the above solution under sonication for at least 2 h to form a homogeneous catalyst ink solution. After that, 20 μL ink solution was carefully coated onto a glassy carbon electrode (GC, 5 mm in diameter). And it was finally dried in the air naturally to obtain a uniform thin film. The catalyst loadings were ~0.36 mg cm⁻². The commercial activated carbon (AC), MCNAs and commercial Pt/C (20 wt% Pt on carbon black) were also employed to prepare the working electrode at the same condition for comparison.

Preparation of air catalytic electrode: Firstly, acetylene black (AB) and poly (tetrafluoroethylene) (PTFE) binder was dispersed in isopropanol to form slurry with a weight ration of 6:4 (AB: PTFE). Next, the slurry (AB + PTFE) was rolled into a membrane with a diameter of 14 mm, and then slightly pressed on the Ni foam to form waterproof layer under the pressure of 5 MPa. After that, with the same way, the slurry (catalyst+AB+PTFE) was rolled into a membrane with a weight ration of 8:1:1 (catalyst: AB: PTFE) and then pressed on the surface of the waterproof layer under the pressure of 40MPa to form air catalytic cathode. The total mass loading of catalyst in the air cathode is around 1.5~2.0 mg/cm². The coated electrode was dried for 12 h at 120 °C under vacuum to remove residual solvent.

Preparation of Zn–Air Batteries: Zn-air batteries were assembled with a home-made Zn–air cell using a prepared catalyst cathode. The battery performance was evaluated by continuous discharge–charge experiments performed under ambient air conditions

(oxygen supplied only from the environment, without additional O₂ sources) using an alkaline aqueous electrolyte of 6 M KOH and a polished zinc plate as the anode. All of the results for the current densities were calculated with the mass loading of catalyst. LAND cycler (Wuhan Land Electronic Co. Ltd.) was used for electrochemical investigation.

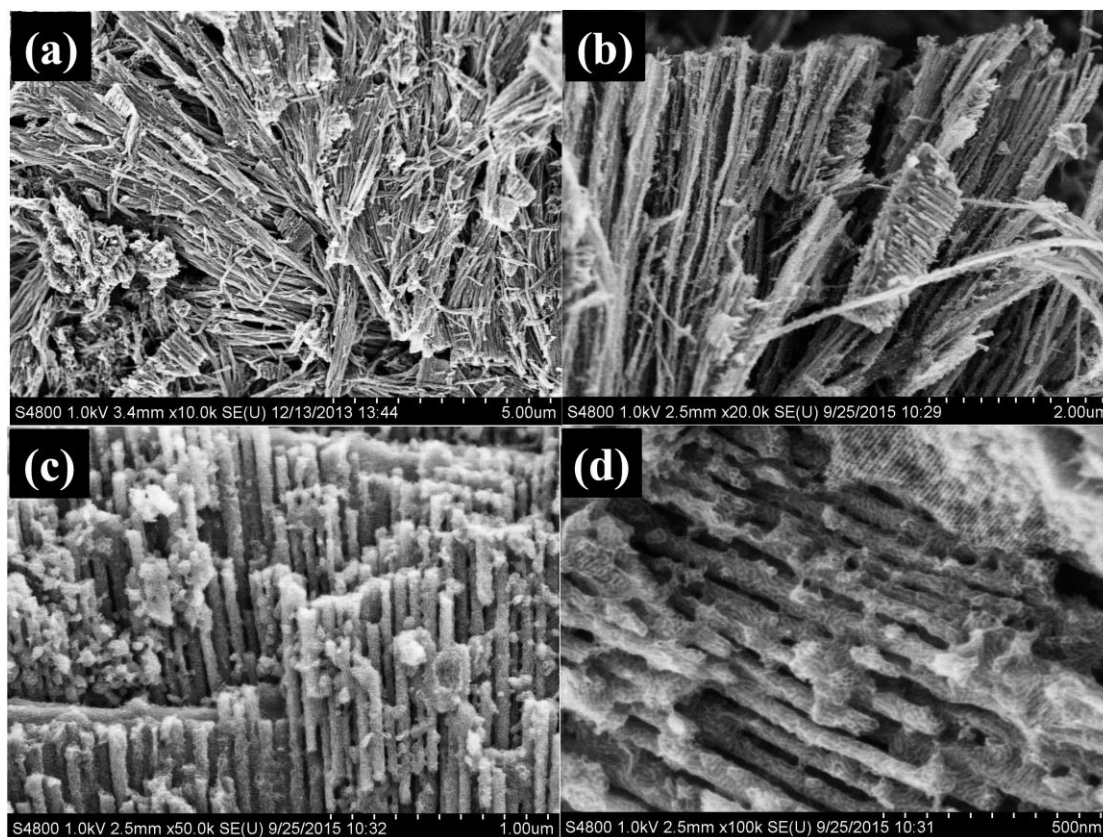


Fig. S1 SEM images of MCNAs with different magnifications. As shown in **Fig. S1**, morphology of as-prepared MCNAs is quite similar to the structure of the crab shell template, suggesting a faithful replication [see our previous publication (ref.46, *J. Mater. Chem.* 2010, 20, 4223-4230)]. In addition, carbon nanofibers are closely packed into ordered arrays in a wide region and notable ordered mesopores are detected throughout the skeleton. Moreover, there are a lot of the void pores formed between the nanofibers with a diameter of approximately 75 nm (see **Fig.S1c** and **d**).

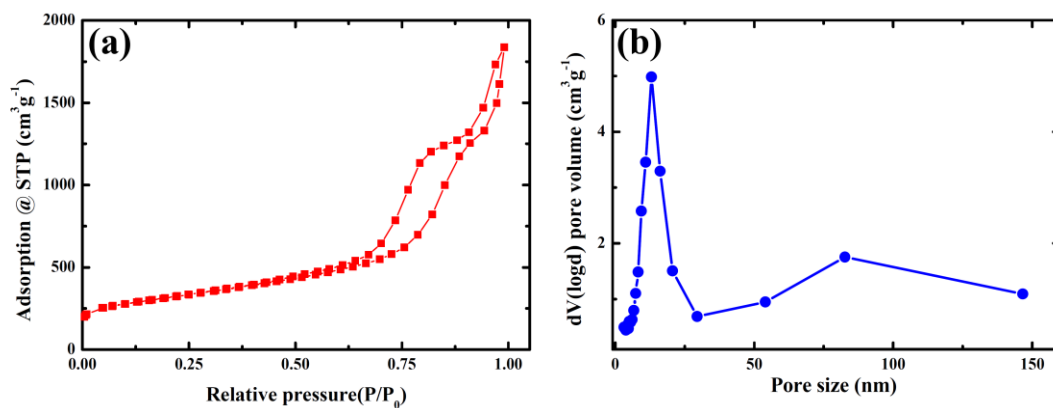


Fig. S2 (a) Nitrogen adsorption-desorption isotherms and (b) pore-size distribution of MCNAs. As shown in **Fig. S2**, the nitrogen adsorption-desorption isotherm of the MCNAs exhibits two substantial hysteresis loops at a relative pressure (P/P_0) range of 0.6–1.0, indicating a hierarchical structure including mesopores and macropores, which is in agreement with the SEM images of MCNAs (**Fig. S1**).

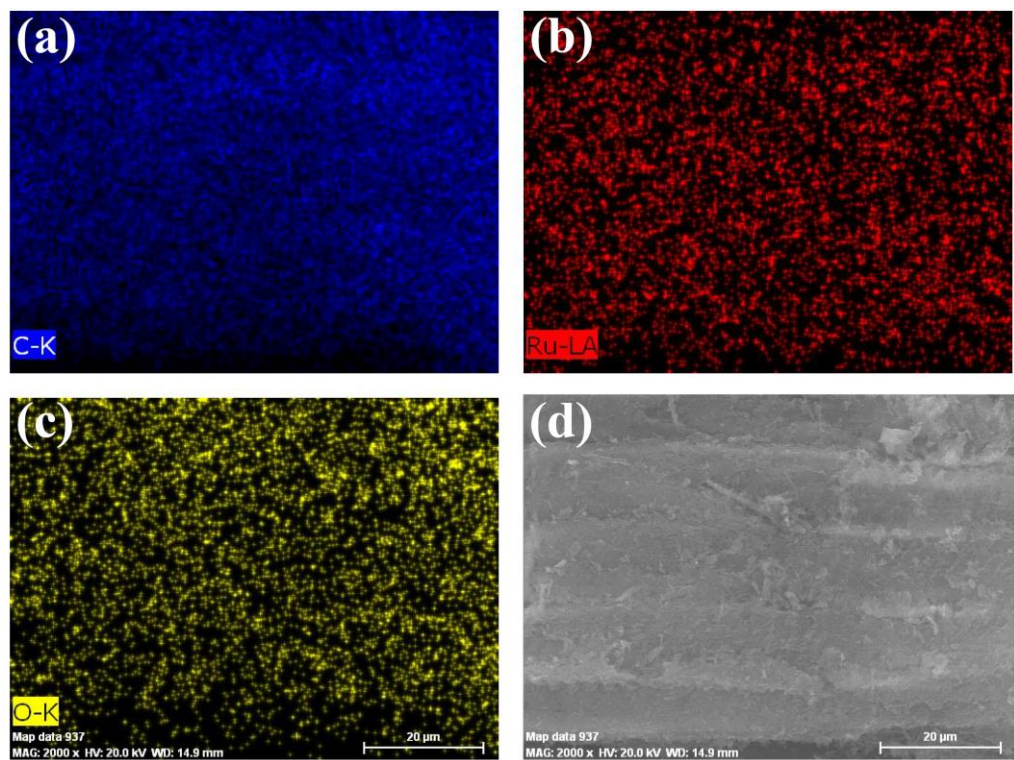


Fig. S3 SEM image of RuO₂-coated MCNAs (bottom right) and the corresponding EDX mapping images of C, Ru and O elements.

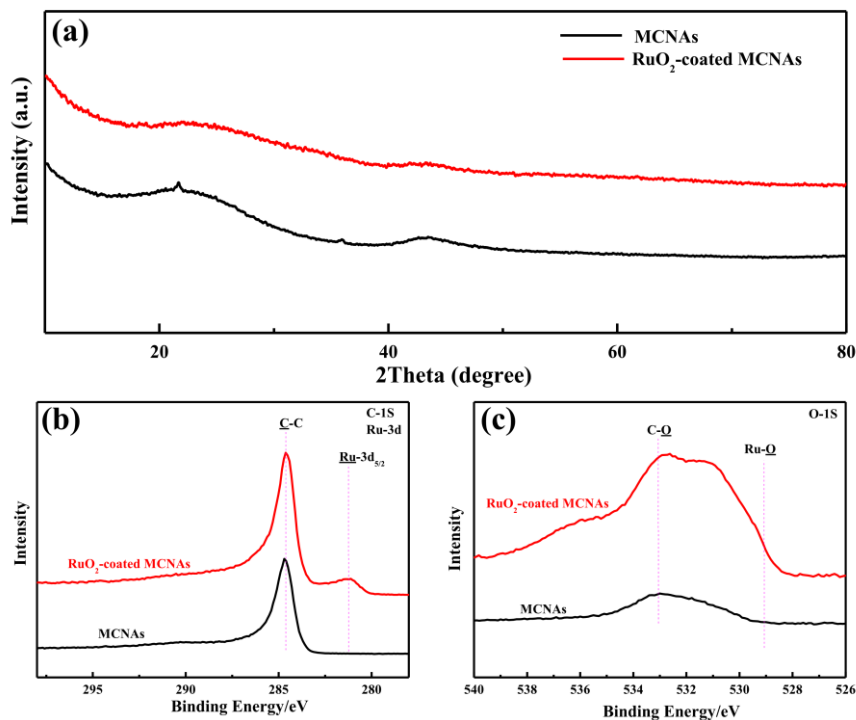


Fig. S4 (a)XRD patterns of MCNAs and RuO₂-coated MCNAs; (b) C 1s & Ru 3d and (c) O 1s XPS spectra of MCNAs and RuO₂-coated MCNAs.

As shown in **Fig. S4a**, the XRD pattern of RuO₂-coated MCNAs is similar to that of bare MCNAs. However, the characteristic peaks related to RuO₂ is hardly observed in RuO₂-coated MCNAs, which indicates that RuO₂ nanoparticles in RuO₂-coated MCNAs is amorphous since less crystalline compounds cannot be detected in the XRD pattern. Therefore, RuO₂-coated MCNAs are further subjected to X-ray photoelectron spectroscopy (XPS) in **Fig. S4b** and **c**. As shown in **Fig. S4b** and **c**, Ru 3d and O 1s high-resolution XPS spectra present peaks at a binding energy of 281 eV and 529 eV for the RuO₂-coated MCNAs, respectively, indicating a large amount of RuO₂ nanoparticles existed in the RuO₂-coated MCNAs (ref. S5 and 6). In addition, the peaks assigned to RuO₂ in the Ru 3d and O 1S XPS spectra cannot be observed in the MCNAs, which further indicates the successful RuO₂ coating in RuO₂-coated MCNAs.

ref. S5: F. J. Li, D. M. Tang, Y. Chen, D. Golberg, H. Kitaura, T. Zhang, A. Yamada and H. S. Zhou, *Nano Lett.*, 2013, **13**, 4702–4707.

ref. S6: Z. Y. Guo, C. Li, J. Y. Liu, X. L. Su, Y. G. Wang and Y. Y. Xia, *J. Mater. Chem. A*, 2015, **3**, 21123–21132.

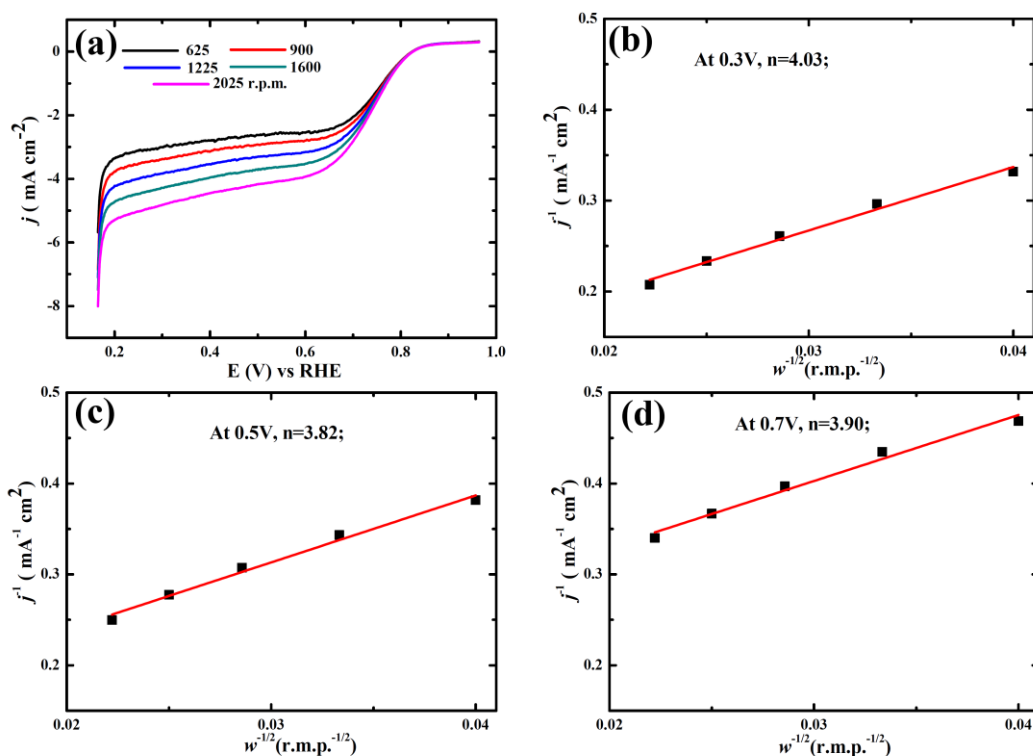


Fig. S5 (a) Linear scan voltammogram (LSV) curves for RuO₂-coated MCNAs in O₂-saturated 0.1M KOH solution at various rotating speeds, scan rate: 5mV s⁻¹; K–L plots for RuO₂-coated MCNAs at various potentials: (b) 0.3V; (c) 0.5V; (d) 0.7V. As shown in **Fig. S5a**, RDE measurements were performed at various rotation rates between 625 rpm to 2025 rpm to understand the ORR kinetics of RuO₂-coated MCNAs. The corresponding Koutecky–Levich (K–L) plots are given in **Fig. S5b~d**. The linearity and near parallelism of the fitting lines suggest a first-order reaction kinetics towards the concentration of dissolved O₂ for RuO₂-coated MCNAs and similar electron transfer number (n) for ORR within a relatively wide electrochemical window. From the K–L equation, the n was calculated to be approximately 4.0 at the potentials between 0.3 to 0.7 V vs RHE (see experimental section for the details), suggesting a 4-electron transfer process for RuO₂-coated MCNAs.

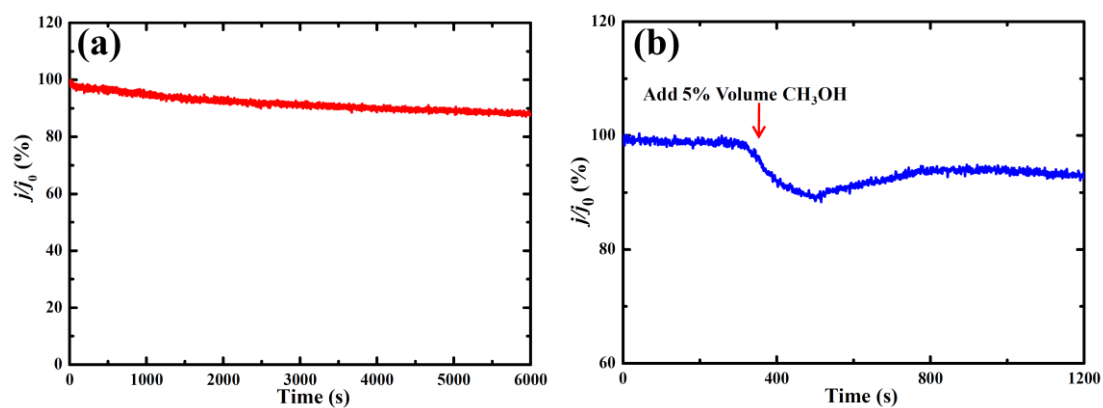


Fig. S6 (a) ORR chronoamperometric response of Pt/C in oxygen-saturated 0.1 M KOH at a constant potential of 0.165 V and (b) ORR chronoamperometric response after methanol addition. The arrow indicates the addition of 5 % volume methanol into the electrochemical cell.

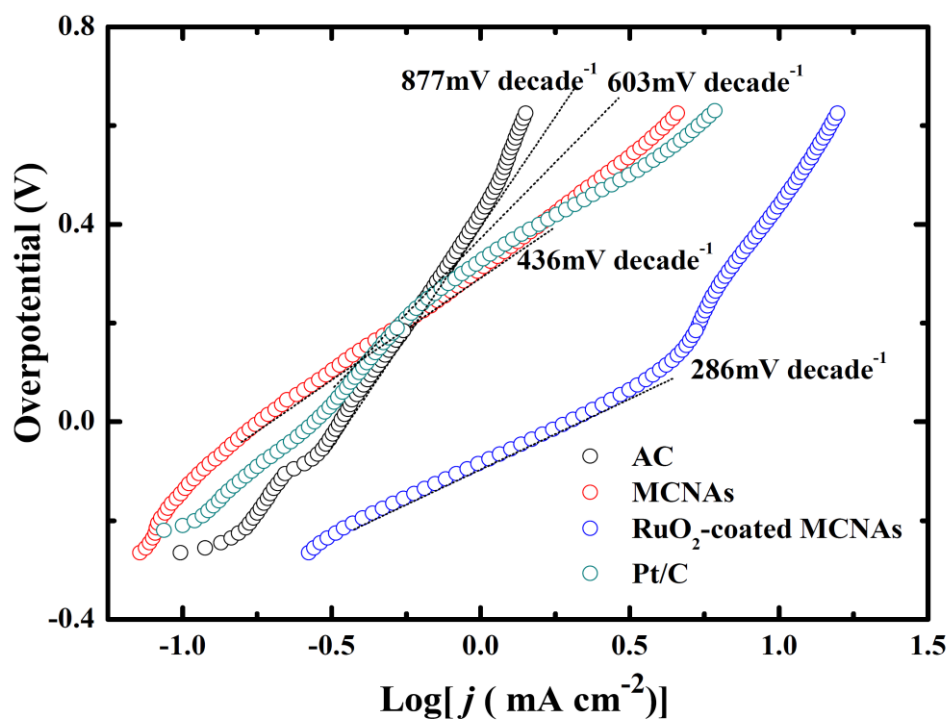


Fig. S7 Tafel plots (b) for AC, MCNAs, RuO₂-coated MCNAs and Pt/C on a RDE (1600 rpm) in an O₂-saturated 0.1 M KOH solution (scan rate: 5 mV s⁻¹). These results indicate that RuO₂-coated MCNAs can enhance the oxygen evolution with a small overpotential. In comparison with AC, MCNAs and Pt/C, the smaller slope suggests the better kinetic process for OER at RuO₂-coated MCNAs.

	$E_{\text{overpotential}}$ /V	Cycle Number	Per Cycle/min	Mass Loading /mg cm ⁻¹	Ref.
NPMC-1000	1.0	600	10	1.5	S7
CCBC-2	1.4	75	/	0.78	S8
A-ECP-900	0.85	160	60	/	S9
Co ₃ O ₄ NC/N-CNT	1.2	25	240	1.0	S10
C-CoPAN900	0.85	55	60	1.0	S11
La _{0.7} -50nm	1.5	8	120	/	S12
c-CoMn ₂ /C	1.0	155	6.7	/	S13
NCNT/CoO-NiO-NiCo	0.86	100	10	0.53	S14
HMC	0.9	100	10	1.0	S15
MCF/N-rGO	1.2	75	4	/	S16
RuO ₂ -coated MCNAs	0.8	80	120	2.0	This work

Tab. S1 Comparison of the rechargeable Zn–air batteries performance of RuO₂-coated MCNAs with various catalysts in the recent literature. As listed in **Tab. S1**, the RuO₂-coated MCNAs catalyst based Zn–air battery shows the lower overpotential, longer cycling time and higher mass loading than other bifunctional catalysts based Zn–air batteries in the recent literatures (ref. S7–16), which further highlights the superior performance and stability of RuO₂-coated MCNAs for Zn–air cells.

References

- ref. S7:** J. T. Zhang, Z. H. Zhao, Z. H. Xia and L. M. Dai, *Nat. Nanotechnol.*, 2015, **10**, 444–452.
- ref. S8:** Z. Chen, A. P. Yu, Y. D. Higgins, H. Li, H. J. Wang and Z. W. Chen, *Nano lett.*, 2012, **12**, 1946–1952.
- ref. S9:** B. Li, D. S. Geng, X. S. Lee, X. M. Ge, J. W. Chai, Z. J. Wang, J. Zhang, Z. L. Liu, T. S. A. Hor and Y. Zong, *Chem. Commun.*, 2015, **51**, 8841–8844.
- ref. S10:** D. U. Lee, M. G. Park, H. W. Park, M. H. Seo and X. L. Wang, *ChemSusChem*, 2015, **8**, 3129-3138.
- ref. S11:** B. Li, X. M. Ge, F. W. T. Goh, T. S. A. Hor, D. S. Geng, G. J. Du, Z. L. Liu, J. Zhang, X. G. Liu and Y. Zong, *Nanoscale*, 2015, **7**, 1830–1838.
- ref. S12:** J. Jung, M. Risch, S. Park, M. G. Kim, G. Nam, Y. Jeong, Y. Shao-Horn and J. Cho, *Energy Environ. Sci.*, 2016, **9**, 176–183.
- ref. S13:** C. Li, X. P. Han, F. Y. Cheng, Y. X. Hu, C. C. Chen and J. Chen, *Nat.*

Commun., 2015, **6**, 7345.

ref. S14: X. Liu, M. Park, M. G. Kim, S. Gupta, G. Wu and J. Cho, *Angew. Chem. Int. Ed.*, 2015, **54**, 9654–9658.

ref. S15: L. Hadidi, E. Davari, M. Iqbal, T. K. Purkait, D. G. Ivey and G. C. Veinot, *Nanoscale*, 2015, **7**, 1830–1838.

ref. S16: Y. Zhan, C. Xu, M. Lu, Z. Liu and J. Y. Lee, *J. Mater. Chem. A*, 2014, **2**, 16217–16223.